Paper

Robust AGC : Traditional Structure Versus Restructured Scheme

Hassan Bevrani* Student Member
Yasunori Mitani** Member
Kiichiro Tsuji* Member

In this paper, a decentralized robust approach is proposed for the Automatic Generation Control (AGC) system based on a modified traditional AGC structure. This work addresses the new strategy to adapt well-tested classical AGC scheme to the changing environment of power system operation under deregulation. The effect of bilateral contracts is considered as a set of new input signals in each control area dynamical model.

In practice, AGC systems use simple proportional-integral (PI) controllers. However, since the PI controller parameters are usually tuned based on classical or trial-and-error approaches, they are incapable of obtaining good dynamical performance for a wide range of operating conditions and various scenarios in deregulated environment. In this paper with regard to this problem, the AGC synthesis is formulated as an H_∞ static output control problem and is solved using a developed iterative linear matrix inequalities (ILMI) algorithm to design of robust PI controllers in the restructured power system control areas. A three area power system example with possible contract scenarios and wide range of load changes is given to illustrate the proposed approach. The resulting controllers are shown to minimize the effect of disturbances and maintain the robust performance.

Keywords: Automatic generation control, H_∞ control, restructured power system, linear matrix inequalities, bilateral contracts

1. Introduction

Currently, the electric power industry is in transition from large, vertically integrated utilities providing power at regulated rates to an industry that will incorporate competitive companies selling unbundled power at lower rates. In a deregulated environment, automatic generation control (AGC) acquires a fundamental role to enable power exchanges and to provide better conditions for the electricity trading. AGC is treated as an ancillary service essential for maintaining the electrical system reliability at an adequate level [(1)].

Several control scenarios based on robust and optimal approaches have been proposed for AGC system in deregulated power system. Some research works on AGC in restructured power system are contained in Ref. (2)∼(14). But the most of them suggest complex state-feedback or high-order dynamic controllers, which are not practical for industry practices. Furthermore, some references have used the untested AGC frameworks, which may have some difficulties to implement in real-world power systems. Usually, the existing AGC systems in the practical power systems use the proportional-integral (PI) type controllers that are tuned online based on classical and trial-and-error approaches. A method for PI control design is reported in Ref. (15), which used a combination of H_∞ control and genetic algorithm techniques for tuning the PI parameters. Also, Ref. (16) has given the sequential decentralized method to obtain a set of low order robust controllers, but both of them are applied for traditional AGC structures. Recently, several reported strategies attempted to adapt well tested classical AGC schemes to the changing environment of power system operation under deregulation [(17)∼(20)].

In this paper, first we introduce a modified dynamical model for a general control area in the deregulated environment, following the ideas presented in Ref. (18)∼(20). This model will show how the bilateral contracts are incorporated in the traditional AGC system leading to a new model. Then the AGC problem will be formulated as an H_∞ control problem to obtain the proportional-integral (PI) controller via the static output feedback control design. An iterative linear matrix inequalities (ILMI) algorithm is developed to compute PI parameters.

The proposed strategy is applied to a three control area example. The obtained robust PI controllers, which are ideally practical for industry, will be compared with the H_∞ dynamic output feedback controllers (using general LMI technique). The results show the controllers guarantee the robust performance for a wide range of operating conditions as well as full-dynamic H_∞ controllers. This paper is organized as follows: Section 2 describes the modified traditional AGC structure versus

* Department of Electrical Eng., Graduate School of Eng., Osaka University
2-1, Yamada-Oka, Suita 565-0871
** Department of Electrical Eng., Kyushu Institute of Technology
1-1, Sensuicho Tobata-ku, Kitakyushu 804-8550

new environment. Technical background on H_∞ static output feedback control is given in section 3. Section 4 presents the proposed strategy including problem formulation, dynamical model and developed ILMI algorithm. The proposed methodology is applied to a three-area power system as a case study, in section 5. Finally to demonstrate the effectiveness of the proposed method, some simulation results for a set of various contract scenarios are given in section 6.

2. Traditional AGC Versus New Structure

2.1 Traditional AGC The traditional AGC is well discussed in Ref. (21) (22). In a traditional power system structure, the generation, transmission and distribution is owned by a single entity called vertically integrated utility (VIU) which supplies power to the customers at regulated rates. Usually the definition of a control area is determined by the physical boundaries of a VIU. All such control areas are interconnected by tie lines. In the classical AGC system, the balance between connected areas is achieved by detecting the frequency and tie line power deviations to generate the area control error (ACE) signal which is turn utilized in the PI control strategy as shown in the Fig. 1.

where

Δf_i: frequency deviation, ΔP_{gi}: governor valve position, ΔP_{ci}: governor load setpoint, ΔP_{ti}: turbine power, ΔP_{tie-i}: net tie-line power flow, ΔP_{di}: area load disturbance, M_i: equivalent inertia constant, D_i: equivalent damping coefficient, T_{gi}: governor time constant, T_{ti}: turbine time constant, T_{ij}: tie-line synchronizing coefficient between area i & j, B_i: frequency bias and R_i: drooping characteristic.

In Fig. 1, w_{1i} and w_{2i} can be defined as follows. Considering these input signals as two disturbance channels is useful with regards to decentralized controller design [16].

$$w_{1i} = \Delta P_{di} \quad \cdots\cdots (1)$$

$$w_{2i} = \sum_{\substack{j=1 \\ j\neq i}}^{N} T_{ij}\Delta f_j \quad \cdots\cdots (2)$$

Following a load disturbance within an area, the frequency of that area, experiences a transient change and the feedback mechanism comes into play and generates

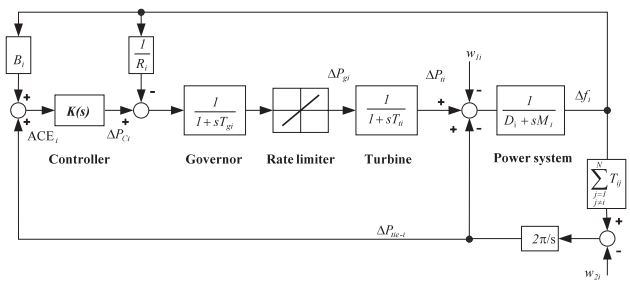

Fig. 1. A control area: Traditional structure

appropriate rise/lower signal to the turbine to make generation follow the load. In the steady state, the generation is matched with the load, driving the tie-line power and frequency deviations to zero. This control structure has performed exceedingly well in the past.

2.2 Modified AGC Here, we introduce a modified dynamical model for AGC analysis and synthesis in the new environment versus traditional one, following the ideas presented in Ref. (18)∼(20). In a restructured power system, VIU no longer exist, however the common objectives, i.e. restoring the frequency and the net interchanges to their desired values for each control area are remained. The new AGC model will need all the information required in a vertically operated utility industry plus the contract data information. The new power system structure includes separate generation, transmission and distribution companies with an open access policy. Based on bilateral transactions, a distribution company (Disco) has the freedom to contract with any available generation company (Genco) in its own or another control area. Therefore the concept of physical control area is replaced by virtual control area (VCA). The boundary of the VCA is flexible and encloses the Gencos and the Disco associated with the contract. In a full bilateral AGC framework, each Disco is responsible for tracking its own load and honoring tie-line power exchange contracts with its neighbors by securing as much transmission and generation capacity as needed.

Analogously to the traditional AGC the physical control area boundaries are assumed for each Disco, its distribution area and local Gencos as before. But the Disco may have a contract with a Genco in out of its distribution area boundaries, in another control area. Similar to Ref. (2), the general theme in our paper is that the loads (the Discos) are responsible for purchasing the services they require. Each control area has its own AGC and is responsible for tracking its own load and honoring tie-line power exchange contracts with its neighbors. All the transactions have to be cleared by the ISO or other responsible organization. There can be various combinations of contracts between each Disco and available Gencos. On the other hand each Genco can contract with various Discos. Similar to the Disco participation matrix in Ref. (20), let define the "generation participation matrix (GPM)" concept to conveniently visualize of these bilateral contracts.

GPM shows the participation factor of each Genco in the considered control areas and each control area is determined by a Disco. The rows of a GPM correspond to Gencos and columns to control areas which contract power. For example, for a large scale power system with m control area (Discos) and n Gencos, the GPM has the following structure.

$$GPM = \begin{bmatrix} gpf_{11} & gpf_{12} & \cdots & gpf_{1(m-1)} & gpf_{1m} \\ gpf_{21} & gpf_{22} & \cdots & gpf_{2(m-1)} & gpf_{2m} \\ \vdots & \vdots & \vdots & \vdots & \vdots \\ gpf_{(n-1)1} & gpf_{(n-1)2} & \cdots & gpf_{(n-1)(m-1)} & gpf_{(n-1)m} \\ gpf_{n1} & gpf_{n2} & \cdots & gpf_{n(m-1)} & gpf_{nm} \end{bmatrix} \quad \cdots\cdots (3)$$

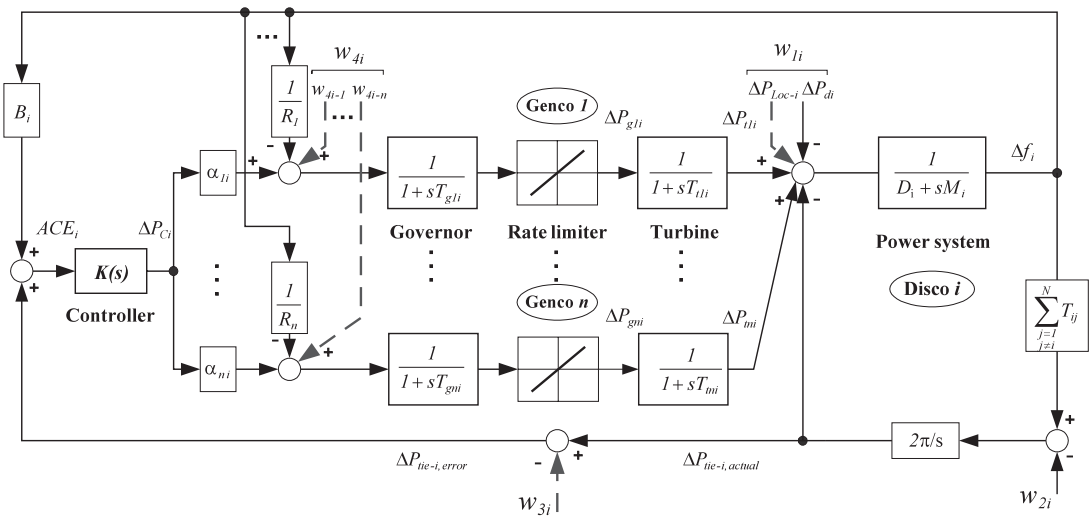

Fig. 2. Modified control area in a deregulated environment

Where gpf_{ij} refers to "generation participation factor" and shows the participation factor of Genco i in the load following of area j (based on a specified bilateral contract). The sum of all the entries in a column in this matrix is unity, e.g.

$$\sum_{i=1}^{n} gpf_{ij} = 1 \cdots\cdots (4)$$

Any entry in a *GPM* that corresponds to a contracted load by a Disco, demanded from the corresponding Genco, must be reflected to the control area system. This introduces new information signals which were absent in the traditional structure. These signals identify which Genco has to follow a load demanded by a specified Disco. The scheduled flow over the tie lines must be adjusted by demand signals of those distribution control areas having a contract with Gencos out of its boundaries. The difference between scheduled and current (actual) tie-line power flows gives a tie-line power error which is used to perform area control error (ACE) signal.

Based on above explanations, the modified AGC block diagram for control area i will be obtained in a deregulated environment as shown in Fig. 2. New information signals due to possible various contracts between Disco i and other Discos and Gencos are shown as dashed-line inputs. Where,

$$\sum_{k=1}^{n} \alpha_{ki} = 1; \quad 0 \le \alpha_{ki} \le 1 \cdots\cdots (5)$$

$$w_{1i} = \Delta P_{Loc-i} + \Delta P_{di} \cdots\cdots (6)$$

$$w_{3i} = \sum (\textit{Total export power} - \textit{Total import power})$$

$$= \sum_{\substack{j=1 \\ j\neq i}}^{N} \left(\sum_{k=1}^{n} gpf_{kj} \right) \Delta P_{Lj} - \sum_{k=1}^{n} \left(\sum_{\substack{j=1 \\ j\neq i}}^{N} gpf_{jk} \right) \Delta P_{Li} \cdots\cdots (7)$$

$$\Delta P_{tie-i,error} = \Delta P_{tie-i,actual} - w_{3i} \cdots\cdots (8)$$

$$\begin{aligned} w_{4i-1} &= \sum_{j=1}^{N} gpf_{1j} \Delta P_{Lj} \\ &\vdots \\ w_{4i-n} &= \sum_{j=1}^{N} gpf_{nj} \Delta P_{Lj} \end{aligned} \cdots\cdots (9)$$

and,

α: ACE participation factor, N: number of control areas, ΔP_{Li}: contracted demand of area i, ΔP_{Loc-i}: total local demand (contracted and uncontracted) in area i, w_{3i}: scheduled $\Delta P_{tie-i}(\Delta P_{tie-i,scheduled})$ and $\Delta P_{tie-i,actual}$: actual ΔP_{tie-i}.

The input w_{2i} is defined as traditional form Eq. (2). The generation of each Genco must track the contracted demands of Discos in steady state. The desired total power generation of Genco i in terms of GPM entries can be calculated as

$$\Delta P_{mi} = \sum_{j=1}^{N} gpf_{ij} \Delta P_{Lj} \cdots\cdots (10)$$

In order to taken account the contract violation cases, as like as Ref. (18), the excess demand by a distribution area (Disco) is not contracted out to any Genco and the load change appears only in terms of its ACE and its shared by all the Gencos of the area (in which the contract violation occurs). The validity of above model will be cleared using some simulation scenarios in section 6.

3. H_∞ Static Output Feedback: Technical Background

This section gives a brief overview on H_∞ static output feedback controller design. Consider a linear time invariant system $G(s)$ with the following state-space realization

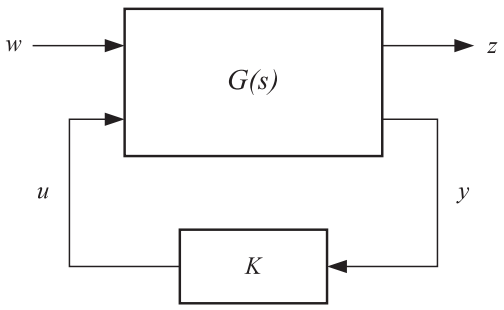

Fig. 3. Closed-loop system via H_∞ control

$$\begin{aligned} \dot{x} &= Ax + B_1 w + B_2 u \\ z &= C_1 x + D_{12} u \cdots\cdots (11) \\ y &= C_2 x \end{aligned}$$

where x is the state variable vector, w is the disturbance and other external input vector, z is the controlled output vector and y is the measured output vector.

The H_∞ static output control problem is to find a static output feedback $u = Ky$, as shown in Fig. 3, such that the resulting closed-loop system is internally stable, and the H_∞ norm from w to z is smaller than γ, a specified positive number, i.e.

$$\|T_{zw}(s)\|_\infty < \gamma \cdots\cdots (12)$$

Theorem 1. It is assumed (A, B_2, C_2) is stabilizable and detectable. The matrix K is an H_∞ controller, if and only if there exists a symmetric matrix $X > 0$ such that

$$\begin{bmatrix} A_{cl}^T X + X A_{cl} & X B_{cl} & C_{cl}^T \\ B_{cl}^T X & -\gamma I & D_{cl}^T \\ C_{cl} & D_{cl} & -\gamma I \end{bmatrix} < 0 \cdots\cdots (13)$$

Where

$$\begin{aligned} A_{cl} &= A + B_2 K C_2, \quad B_{cl} = B_1 \\ C_{cl} &= C_1 + D_{12} K C_2, \quad D_{cl} = 0 \end{aligned}$$

The proof is given in Ref. (23) (24). We can rewrite Eq. (13) as following matrix inequality [25],

$$\overline{XB} K \bar{C} + (\overline{XB} K \bar{C})^T + \bar{A}^T \bar{X} + \overline{XA} < 0 \cdots (14)$$

where

$$\left.\begin{aligned} \bar{A} &= \begin{bmatrix} A & B_1 & 0 \\ 0 & -\gamma I/2 & 0 \\ C_1 & 0 & -\gamma I/2 \end{bmatrix} \\ \bar{B} &= \begin{bmatrix} B_2 \\ 0 \\ D_{12} \end{bmatrix} \\ \bar{C} &= \begin{bmatrix} C_2 & 0 & 0 \end{bmatrix} \end{aligned}\right\} \cdots\cdots (15)$$

and,

$$\bar{X} = \begin{bmatrix} X & 0 & 0 \\ 0 & I & 0 \\ 0 & 0 & I \end{bmatrix}.$$

Hence, the H_∞ static output feedback control problem is reduced to find $X > 0$ and K such that matrix inequality Eq. (14) holds. In fact it is a generalized static output feedback stabilization problem of the system $(\bar{A}, \bar{B}, \bar{C})$, which can be solved via the following theorem.

Theorem 2. The system (A, B, C) that may also be identified by the following representation,

$$\left.\begin{aligned} \dot{x} &= Ax + Bu \\ y &= Cx \end{aligned}\right\} \cdots\cdots (16)$$

is stabilizable via static output feedback if and only if there exist $P > 0$, $X > 0$ and K satisfying the following quadratic matrix inequality

$$\begin{bmatrix} A^T X + XA - PBB^T X - XBB^T P + PBB^T P & (B^T X + KC)^T \\ B^T X + KC & -I \end{bmatrix} < 0 \cdots\cdots (17)$$

Proof. According to the Schur complement, the quadratic matrix inequality Eq. (17) is equivalent to the following matrix inequality

$$\begin{aligned} &A^T X + XA - PBB^T X - XBB^T P + PBB^T P \\ &\quad + (B^T X + KC)^T (B^T X + KC) < 0 \cdots\cdots (18) \end{aligned}$$

For this new inequality notation Eq. (18), the sufficiency and necessity of theorem are already proven. Please see Ref. (26).

4. Proposed Strategy

4.1 Problem Statement and Modeling A large scale power system consists of a number of interconnected distribution control areas that each control area has a Disco and one or more Gencos (Fig. 2). As shown in Fig. 1, the ACE performs the input signal of PI controller which is practically used by the traditional AGC system. Therefore we have

$$u_i = \Delta Pci = k_{Pi} ACE_i + k_{Ii} \int ACE_i \cdots\cdots (19)$$

By augmenting the system description to include the ACE and its integral as the measured output vector, the PI control problem becomes one of finding a static output feedback that satisfied the prescribed performance requirements. Using this strategy, the PI-based AGC design can be reduced to an H_∞ static output feedback problem as shown in Fig. 4. In order to change Eq. (19) to a simple static feedback control as

$$u_i = K_i y_i \cdots\cdots (20)$$

We can rewrite Eq. (19) as follows [15].

$$u_i = [k_{Pi} \ k_{Ii}] \begin{bmatrix} ACE_i \\ \int ACE_i \end{bmatrix} \cdots\cdots (21)$$

Here, to synthesis the H_∞ static output feedback controller an iterative LMI (ILMI) algorithm is proposed using the generalized static output feedback stabilization problem (Theorem 2).

The proposed control framework in order to design of PI controller via the H_∞ static output feedback problem for a given control area is shown in Fig. 5. $G_i(s)$

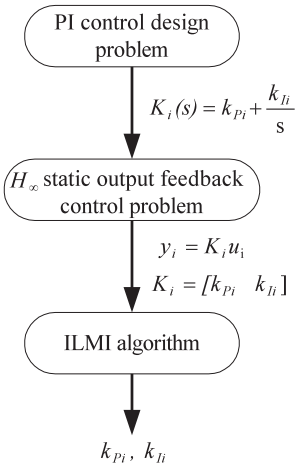

Fig. 4. Problem formulation

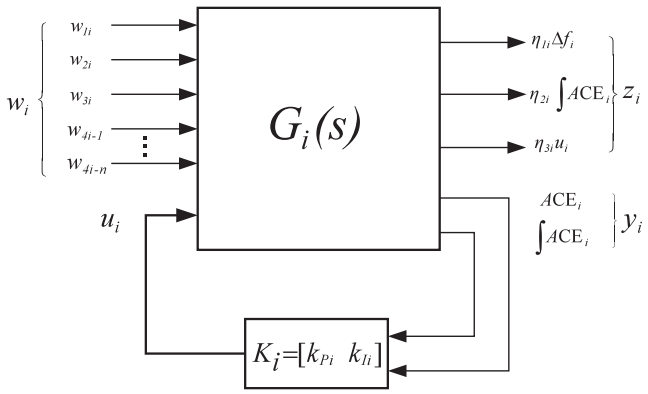

Fig. 5. Proposed control framework

denotes the dynamical model corresponds to modified control area shown in Fig. 2. According to Eq. (11), the state space model for each control area can be obtained as

$$\left.\begin{aligned} \dot{x}_i &= A_i x_i + B_{1_i} w_i + B_{2i} u_i \\ z_i &= C_{1i} x_i + D_{12i} u_i \\ y_i &= C_{2i} x_i \end{aligned}\right\} \cdots\cdots\cdots\cdots\cdots \quad (22)$$

where

$$\left.\begin{aligned} x_i^T &= \begin{bmatrix} \Delta f_i & \Delta P_{tie-i} & \int ACE_i & x_{ti} & x_{gi} \end{bmatrix} \\ x_{ti} &= \begin{bmatrix} \Delta P_{t1i} & \Delta P_{t2i} & \cdots & \Delta P_{tni} \end{bmatrix} \\ x_{gi} &= \begin{bmatrix} \Delta P_{g1i} & \Delta P_{g2i} & \cdots & \Delta P_{gni} \end{bmatrix} \end{aligned}\right\} \cdots\cdots\cdots\cdots\cdots\cdots \quad (23)$$

$$y_i^T = \begin{bmatrix} ACE_i & \int ACE_i \end{bmatrix}, \quad u_i = \Delta P_{Ci} \cdots\cdots \quad (24)$$

$$z_i^T = \begin{bmatrix} \eta_{1i}\Delta f_i & \eta_{2i}\int ACE_i & \eta_{3i} u_i \end{bmatrix} \cdots\cdots\cdots \quad (25)$$

$$w_i^T = [w_{1i} \; w_{2i} \; w_{3i} \; w_{4i} \;]$$

$$w_{4i}^T = [w_{4i-1} \; w_{4i-2} \; \cdots \; w_{4i-n}]$$

and,

$$A_i = \begin{bmatrix} A_{i11} & A_{i12} & A_{i13} \\ A_{i21} & A_{i22} & A_{i23} \\ A_{i31} & A_{i32} & A_{i33} \end{bmatrix}$$

$$B_{1i} = \begin{bmatrix} B_{1i11} & B_{1i12} \\ B_{1i21} & B_{1i22} \\ B_{1i31} & B_{1i32} \end{bmatrix}$$

$$B_{2i} = \begin{bmatrix} B_{2i1} \\ B_{2i2} \\ B_{2i3} \end{bmatrix}$$

$$C_{1i} = [c_{1i} \; 0_{3\times n} \; 0_{3\times n}]$$

$$c_{1i} = \begin{bmatrix} \eta_{1i} & 0 & 0 \\ 0 & 0 & \eta_{2i} \\ 0 & 0 & 0 \end{bmatrix}$$

$$D_{12i} = \begin{bmatrix} 0 \\ 0 \\ \eta_{3i} \end{bmatrix}$$

$$C_{2i} = [c_{2i} \; 0_{2\times n} \; 0_{2\times n}]$$

$$c_{2i} = \begin{bmatrix} B_i & 1 & 0 \\ 0 & 0 & 1 \end{bmatrix}$$

$$A_{i11} = \begin{bmatrix} -D_i/M_i & -1/M_i & 0 \\ 2\pi \sum_{\substack{j=1 \\ j\neq i}}^{N} T_{ij} & 0 & 0 \\ B_i & 1 & 0 \end{bmatrix}$$

$$A_{i12} = \begin{bmatrix} 1/M_i & \cdots & 1/M_i \\ 0 & \cdots & 0 \\ 0 & \cdots & 0 \end{bmatrix}_{3\times n}$$

$$\begin{aligned} A_{i22} &= -A_{i23} \\ &= diag\,[-1/T_{t1i} \quad -1/T_{t2i} \quad \cdots \quad -1/T_{tni}] \end{aligned}$$

$$A_{i33} = diag\,[-1/T_{g1i} \; -1/T_{g2i} \; \cdots \; -1/T_{gni}]$$

$$A_{i31} = \begin{bmatrix} -1/(T_{g1i}R_{1i}) & 0 & 0 \\ \vdots & \vdots & \vdots \\ -1/(T_{gni}R_{ni}) & 0 & 0 \end{bmatrix}$$

$$A_{i13} = A_{i21}^T = 0_{3\times n}$$

$$A_{i32} = 0_{n\times n}$$

$$B_{1i11} = \begin{bmatrix} -1/M_i & 0 & 0 \\ 0 & -2\pi & 0 \\ 0 & 0 & -1 \end{bmatrix}$$

$$B_{1i21} = B_{1i31} = 0_{n\times 3}$$

$$B_{1i12} = 0_{3\times n}$$

$$B_{1i22} = 0_{n\times n}$$

$$B_{1i32} = diag\,[1/T_{g1i} \quad 1/T_{g2i} \quad \cdots \quad 1/T_{gni}]$$

$$B_{2i1} = 0_{3\times 1}$$

$$B_{2i2} = 0_{n\times 1}$$

$$B_{2i3}^T = [\alpha_{1i}/T_{g1i} \quad \alpha_{2i}/T_{g2i} \quad \cdots \quad \alpha_{ni}/T_{gni}]$$

The η_{1i}, η_{2i} and η_{3i} in Fig. 5 and Eq. (25) are constant weighting coefficients that must be chosen by the designer to get the desired performance.

4.2 Developed ILMI Algorithm A solution for the consequent non convex optimization problem Eq. (17) can not be directly achieved by using general LMI technique. However, the matrix inequality Eq. (17) points to an iterative approach to solve the matrix K and X, namely, if P is fixed, then it reduces to an LMI problem in the unknowns K and X. For this purpose, the following iterative LMI algorithm based on the given approach in Ref. (27) is developed. The key point is to formulate the H∞ problem via a generalized static

output stabilization feedback such that all eigenvalues of (A-BKC) shift towards the left half plane through the reduction of a, a real number, to close to feasibility of Eq. (17).

Theorem 2 gives a set of internally stabilizing static output feedback gains is defined as K_{sof}. But we are looking for the solution of following optimization problem.

Optimization problem: Given an optimal performance index γ, Eq. (12), resulted from applied dynamic output feedback H_∞ control to the control area i which is shown in Fig. 5, determine an admissible static output feedback law

$$u_i = K_i y_i, \quad K_i \in K_{sof} \cdots\cdots\cdots\cdots\cdots\cdots\cdots (26)$$

such that

$$\|T_{ziwi}(s)\|_\infty < \gamma^* \cdots\cdots\cdots\cdots\cdots\cdots\cdots\cdots\cdots (27)$$

where γ^* indicates a lower bound such that the closed-loop system is H_∞ stabilizable via static output feedback. In this case we could see that $|\gamma - \gamma^*| < \varepsilon$, where ε is a small real positive number.

The following algorithm gives an iterative LMI solution for above optimization problem:

Step 1. Perform the new system $(\bar{A}, \bar{B}, \bar{C})$, according to Eq. (15).

Set $i = 1$, $\Delta\gamma = \Delta\gamma_0$ and let $\gamma_i = \gamma_0 > \gamma$. $\Delta\gamma_0$ and γ_0 are positive real numbers.

Step 2. Select $Q > 0$, and solve $\bar{X}$ from the following algebraic Riccati equation

$$\bar{A}^T\bar{X} + \overline{XA} - \overline{XBB}^T\bar{X} + Q = 0 \cdots\cdots\cdots\cdots (28)$$

Set $P_1 = \bar{X}$.

Step 3. Solve the following optimization problem for $\bar{X}_i$, K_i and a_i.

Minimize a_i subject to the bellow LMI constraints:

$$\begin{bmatrix} \bar{A}^T\bar{X}_i + \bar{X}_i\bar{A} - P_i\overline{BB}^T\bar{X}_i - \bar{X}_i\overline{BB}^T P_i + P_i\overline{BB}^T P_i - a_i\bar{X}_i & (\bar{B}^T\bar{X}_i + K_i\bar{C})^T \\ \bar{B}^T\bar{X}_i + K_i\bar{C} & -I \end{bmatrix} < 0 \cdots\cdots\cdots\cdots\cdots\cdots (29)$$

$$\bar{X}_i = \bar{X}_i^T > 0. \cdots\cdots\cdots\cdots\cdots\cdots\cdots\cdots\cdots\cdots (30)$$

Denote a_i^* as the minimized value of a_i.

Step 4. If $a_i^* \le 0$, go to Step 8.

Step 5. For $i > 1$ if $a_{i-1}^* \le 0$, $K_{i-1} \in K_{sof}$ and it is desired H_∞ controller and $\gamma^* = \gamma_i + \Delta\gamma$ indicates a lower bound such that the above system is H_∞ stabilizable via static output feedback.

Step 6. Solve the following optimization problem for $\bar{X}_i$ and K_i:

Minimize trace($\bar{X}_i$) subject to the above LMI constraints (29), (30) with $a_i = a_i^*$. Denote $\bar{X}_i^*$ as the $\bar{X}_i$ that minimized trace($\bar{X}_i$).

Step 7. Set $i = i + 1$ and $P_i = \bar{X}_{i-1}^*$, then go to Step 3.

Step 8. Set $\gamma_i = \gamma_i - \Delta\gamma$, $i = i + 1$. Then do Steps 2 to 4.

The matrix inequalities (29) and (30) give a sufficient condition for the existence of static output feedback controller. The developed algorithm is summarized in Fig. 6. In the next section, two types of robust controllers are developed for each control area in a three-area power system example. The first one is dynamic H_∞ controller based on general LMI approach and the second controller is a PI controller based on H_∞ static output feedback using the developed ILMI algorithm, with the same assumed objectives to achieve desired robust performance.

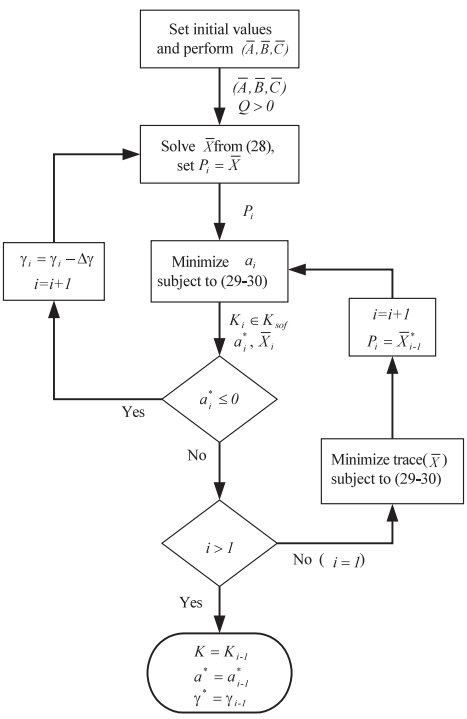

Fig. 6. Developed ILMI algorithm

5. Case Study

To illustrate the effectiveness of modified model and proposed control design, a three control area power system shown in Fig. 7, is considered as a test system. It is assumed that each control area includes two Gencos and one Disco. The power system parameters are tabulated in Table 1 and Table 2. For the simulation tests,

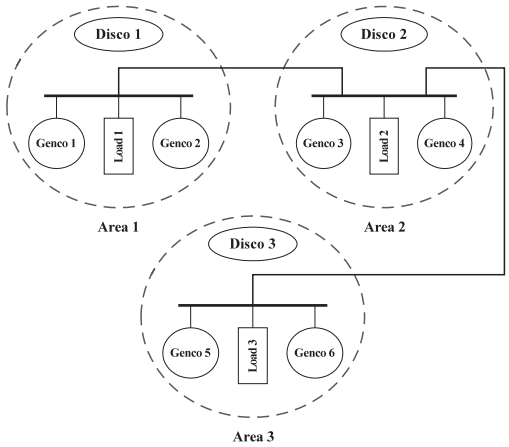

Fig. 7. Three control area power system

Table 1. Applied data for Gencos

Quantity	*Gen -co1*	*Gen -co2*	*Gen -co3*	*Gen -co4*	*Gen -co5*	*Gen -co6*
Rating (MW)	800	1000	1100	1200	1000	1000
R (Hz/pu)	2.4	3.3	2.5	2.4	3	2.4
T_t (sec)	0.36	0.42	0.44	0.4	0. 36	0.4
T_g (sec)	0.06	0.07	0.06	0.08	0.07	0.08
α	0.5	0.5	0.5	0.5	0.5	0.5

Table 2. Applied control area parameters

Quantity	*Area 1*	*Area 2*	*Area 3*
D (pu/Hz)	0.0084	0.014	0.011
M (pu.sec)	0.1667	0.2	0.1667
B (pu/Hz)	0.8675	0.795	0.870
T_{ij} (pu/Hz)	0.545		

the rate limit value for each Genco is assumed 0.1, and, 1000 MW is considered as a base for the *pu* calculations.

For the sake of comparison, for each area, in addition to proposed control strategy to obtain the robust PI controller, a robust H_∞ dynamic output feedback controller is designed using LMI control toolbox. Specifically, based on general LMI first the control design is reduced to a LMI formulation, and then the H_∞ control problem is solved using the function *hinflmi*, provided by the MATLAB's LMI control toolbox [28]. This function gives an optimal H_∞ controller through the minimizing the guaranteed robust performance index Eq. (12) subject to the constraint given by the matrix inequality (13) and returns the controller $K(s)$ with optimal robust performance index.

The selection of constant weights η_{1i}, η_{2i} and η_{3i} is dependent on specified performance objectives and must be chosen by designer. In fact an important issue with regard to selection of these weights is the degree to which they can guarantee the satisfaction of design performance objectives. The selection of these weights entails a trade off among several performance requirements. The coefficients η_{1i} and η_{2i} at controlled outputs set the performance goals e.t. tracking the load variation and disturbance attenuation. η_{3i} sets a limit on the allowed control signal to penalize fast change and large overshoot in the governor load set-point signal. Here, the suitable values for constant weights η_{1i}, η_{2i} and η_{3i} are chosen as 5, 0.5 and 300, respectively.

The resulted controllers using the *hinflmi* function are dynamic type and have the following state-space form, whose orders are the same as size of plant model (7th order in the present paper).

$$\left.\begin{aligned} \dot{x}_{ki} &= A_{ki}x_{ki} + B_{ki}y_i \\ u_i &= C_{ki}x_{ki} + D_{ki}y_i \end{aligned}\right\} \cdots\cdots\cdots\cdots\cdots\cdots \quad (31)$$

At the next step, according to synthesis methodology described in section 4, a set of three decentralized robust PI controllers are designed. As it is mentioned before, this control strategy is fully suitable for AGC applications which usually employ the PI control, while the most of other robust and optimal control designs (such as LMI approach) yield complex controllers whose size can be larger than real-world AGC systems. Using ILMI approach, the controllers are obtained following several iterations. For example, for control area 3 the final result is obtained after 32 iterations. Some iterations are listed in Table 3. The proposed control parameters for three control areas are shown in Table 4.

Table 3. ILMI algorithm result for design of K_3

Iteration	γ	k_{P3}	k_{I3}
1	863.3337	-0.4471	-0.5365
2	863.2084	-0.4456	-0.5363
15	826.0470	-0.2915	-0.0053
22	804.7513	-0.0079	-0.0127
25	800.9137	-0.0672	-0.1236
26	800.8829	-0.1205	-0.2400
27	800.8783	-0.1823	-0.3146
29	800.8770	-0.2095	-0.3525
31	800.8763	-0.2275	-0.3787
32	800.8762	-0.2319	-0.3796

Table 4. Control parameters from ILMI design

Parameters	*Area 1*	*Area 2*	*Area 3*
a^*	-0.3901	-0.2610	-0.0407
k_{Pi}	-0.2695	-0.0418	-0.2319
k_{Ii}	-0.3788	-0.1806	-0.3796

Table 5. Robust performance index

Control design	*Control structure*	*Perf. index*	*Area 1*	*Area 2*	*Area 3*
H∞	9th order	γ	803.0393	801.0699	800.2284
ILMI	PI	γ^*	803.0396	801.0306	800.8762

The resulted robust performance indices of both synthesis methods (γ^* and γ) are too close to each other and given in Table 5. It shows that although the proposed ILMI approach gives a set of much simpler controllers (PI) than the dynamic H_∞ design, however they holds robust performance as well as dynamic H_∞ controllers.

6. Simulation Results

In order to demonstrate the effectiveness of the proposed strategy, some simulations were carried out. In these simulations, the proposed controllers were applied to the three control area power system described in Fig. 7. In this section, the performance of the closed-loop system using the robust PI controllers in comparison of designed dynamic H_∞ controllers is tested for the various possible scenarios of bilateral contracts and load disturbances.

<u>*Scenario 1:*</u>

A large load disturbance (a step increase in demand) is applied to each area:

$$\Delta P_{L1} = 100\,\text{MW},\ \Delta P_{L2} = 70\,\text{MW},\ \Delta P_{L3} = 60\,\text{MW}$$

Assume each Disco demand is sent to its local Gencos only, based on the following GPM

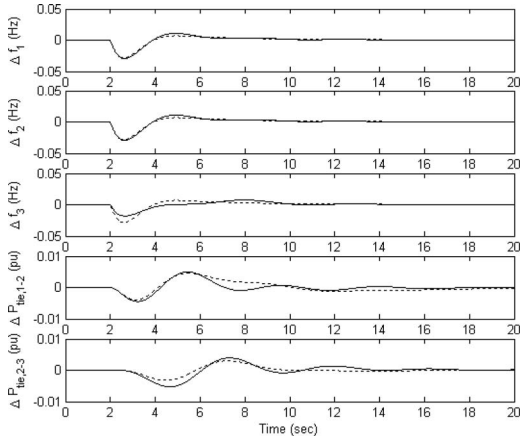

Fig. 8. Frequency deviation and tie-line power changes; solid (ILMI), dotted (LMI)

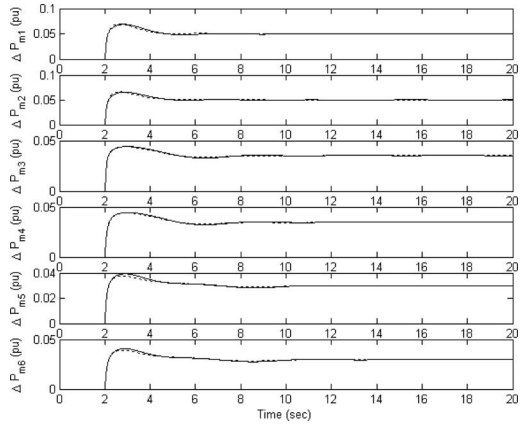

Fig. 9. Mechanical power changes; solid (ILMI), dotted (LMI)

$$GPM = \begin{bmatrix} 0.5 & 0 & 0 \\ 0.5 & 0 & 0 \\ 0 & 0.5 & 0 \\ 0 & 0.5 & 0 \\ 0 & 0 & 0.5 \\ 0 & 0 & 0.5 \end{bmatrix}.$$

Frequency deviation (Δf), tie-line power flow (ΔP_{tie}), power changes (ΔP_m), area control error (ACE) and its integral are shown in Figs. 8∼10 for the closed-loop system. Using the proposed method (ILMI), the area control error and frequency deviation of all areas are quickly driven back to zero, the generated power and tie-line power are properly convergence to specified values, as well as dynamic H_∞ control (LMI).

Since there are no contracts between areas, the scheduled steady state power flows Eq. (7) over the tie lines are zero. The actual tie-line powers are shown in Fig. 8. As it is seen from Fig. 9, the actual generated powers of Gencos, according to Eq. (10), reach the desired values in the steady state.

$$\begin{aligned}\Delta P_{m1} &= gpf_{11}\Delta P_{L1} + gpf_{12}\Delta P_{L2} + gpf_{13}\Delta P_{L3} \\ &= 0.5(0.1) + 0 + 0 = 0.05\,\text{pu}\end{aligned}$$

and,

$$\Delta P_{m2} = 0.05\,\text{pu},\ \Delta P_{m3} = \Delta P_{m4} = 0.035\,\text{pu},$$
$$\Delta P_{m5} = \Delta P_{m6} = 0.03\,\text{pu}.$$

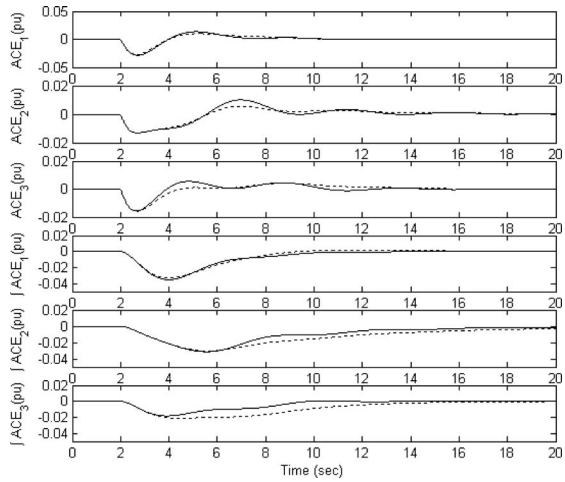

Fig. 10. ACE and its integral; solid (ILMI), dotted (LMI)

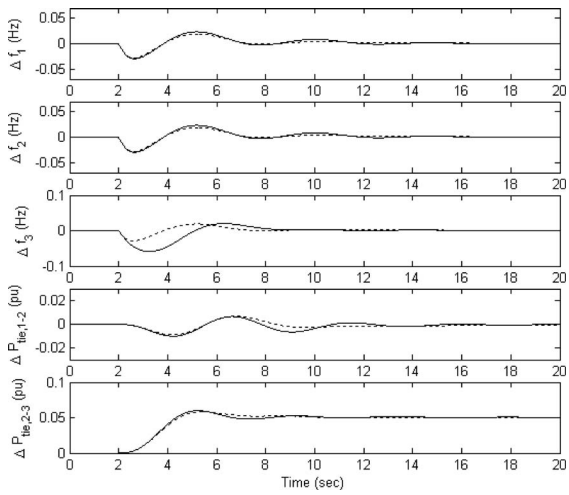

Fig. 11. Frequency deviation and tie-line power changes; solid (ILMI), dotted (LMI)

Scenario 2:

Consider larger demands by Disco 2 and Disco 3, i.e.

$$\Delta P_{L1} = 100\,\text{MW}, \quad \Delta P_{L2} = 100\,\text{MW},$$
$$\Delta P_{L3} = 100\,\text{MW}$$

And assume Discos contract with the available Gencos in other areas, according to the following GPM,

$$GPM = \begin{bmatrix} 0.25 & 0.25 & 0 \\ 0.5 & 0 & 0 \\ 0 & 0.25 & 0.75 \\ 0.25 & 0.25 & 0 \\ 0 & 0.25 & 0 \\ 0 & 0 & 0.25 \end{bmatrix}$$

The closed-loop responses are shown in Figs. 11∼13. According to Eq. (10), the actual generated powers of Gencos for this scenario can be obtained as

$$\Delta P_{m1} = 0.25(0.1) + 0.25(0.1) + 0 = 0.05\,\text{pu}$$

and,

$$\Delta P_{m2} = 0.05\,\text{pu},\ \Delta P_{m3} = 0.1\,\text{pu},$$
$$\Delta P_{m4} = 0.05\,\text{pu},\ \Delta P_{m5} = \Delta P_{m6} = 0.025\,\text{pu}.$$

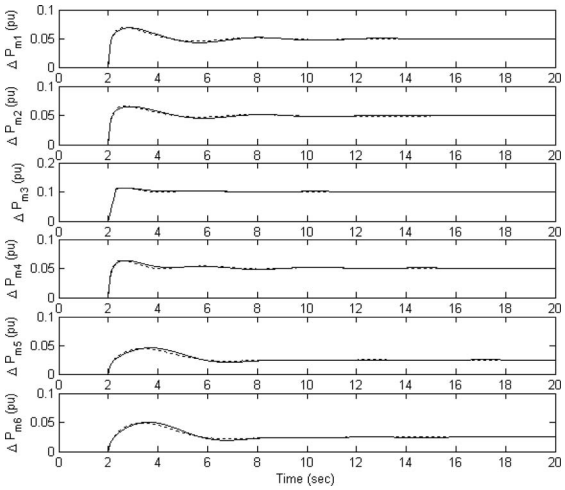

Fig. 12. Mechanical power changes; solid (ILMI), dotted (LMI)

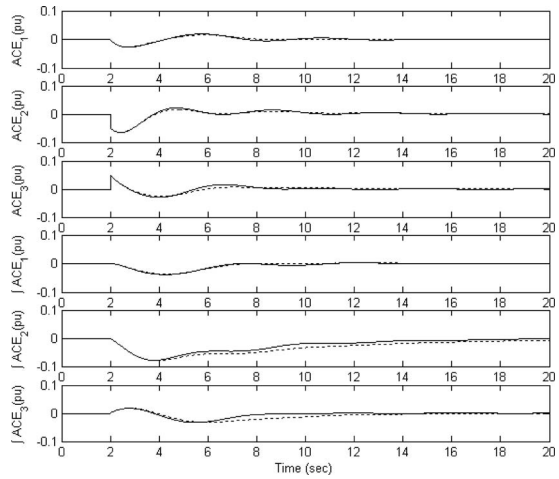

Fig. 13. ACE and its integral; solid (ILMI), dotted (LMI)

The simulation results show the same values in steady state. The scheduled power tie-lines in the directions from area 1 to area 2 and area 2 to area 3, using Eq. (7) are obtained as,

$$\begin{aligned}\Delta P_{tie,1-2} &= (gpf_{12} + gpf_{22})\Delta P_{L2} \\ &\quad - (gpf_{31} + gpf_{41})\Delta P_{L1} \\ &= (0.25 + 0)0.1 - (0 + 0.25)0.1 \\ &= 0\,\text{pu} \\ \Delta P_{tie,2-3} &= (0.75 + 0)0.1 - (0.25 + 0)0.1 \\ &= 0.05\,\text{pu}\end{aligned}$$

Fig. 12 shows the actual tie-line powers and they reach to above values at steady state.

Scenario 3:

In this scenario, we simulate the effect of contract violation problem. Consider the scenario 2 again, but assume the Disco 1 demand 50 MW more power than that specified in the contract. As it is mentioned in section 2, this excess power must be reflected as an uncontracted local demand of area 1 and must be supplied by local Gencos, only. Simulation result is shown in Fig. 14.

Fig. 14 shows the excess load is taken up by Genco 1

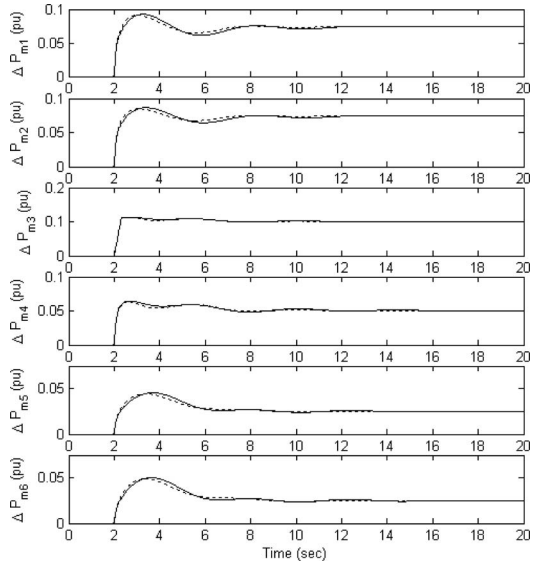

Fig. 14. Generated power in response to contract violation; solid (ILMI), dotted (LMI)

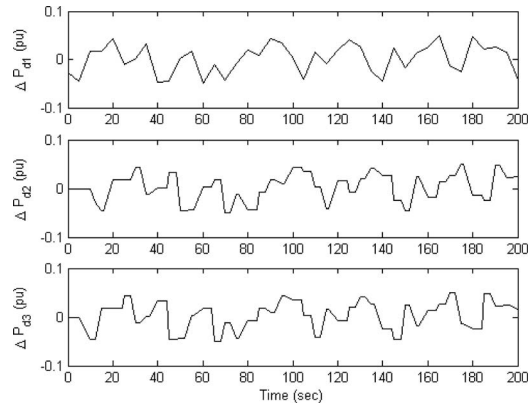

Fig. 15. Random load changes

and Genco 2 only, according to their AGC participation factors, and Gencos in other distribution areas do not participate to compensate it. Since GPM is the same as in scenario 2, the generated power of Gencos in area 2 and area 3 is the same as in scenario 2 in steady state.

Scenario 4:

Consider the conditions of scenario 2 again. Assume in addition to specified contracted demand (100 MW), a bounded random load changes (Fig. 15) as an uncontracted local demand,

$$-50\,\text{MW} \le \Delta P_{di} \le +50\,\text{MW}$$

is applied to each control area. The contract step demands as the same as previous simulation tests are started from 2 sec.

The purpose of this scenario is testing the performance of proposed controllers against large and random load disturbances. The corresponded power changes, frequency deviations and tie-line power flows are shown in Figs. 16 and 17. Finally, Fig. 18 shows ACE and control effort signals for the proposed controllers. These figures demonstrate that the designed controllers track the load fluctuations, effectively.

The simulation results show the proposed PI

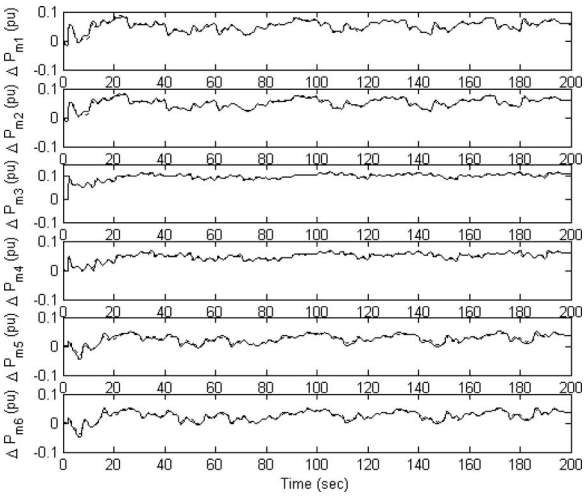

Fig. 16. Generated power in response to scenario 4; solid (ILMI), dotted (LMI)

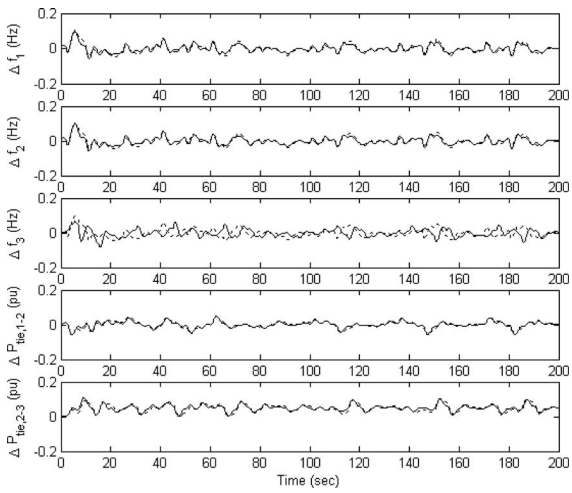

Fig. 17. Frequency deviation and tie-line power flow for scenario 4; solid (ILMI), dotted (LMI)

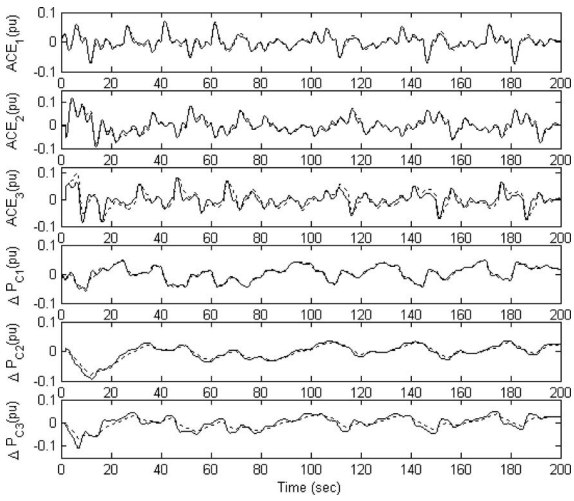

Fig. 18. ACE and control action signals for scenario 4; solid (ILMI), dotted (LMI)

controllers perform robust performance as well as full order dynamic H_∞ controllers (with complex structures) for a wide range of load disturbances and possible bilateral contract scenarios.

7. Conclusion

In this paper a new method for robust decentralized AGC design using an iterative LMI approach has been proposed for a modified traditional AGC system model according to bilateral contracts in the restructured power system. Design strategy includes enough flexibility to setting the desired level of performance, and, gives a set of simple PI controllers, via the H_∞ static output control design, which commonly useful in real-world power systems.

The proposed method was applied to a three control area power system and is tested with four different possible scenarios. The results are compared with the results of applied dynamic H_∞ output controllers. Simulation results demonstrated the effectiveness of methodology. It was shown that the designed controllers are capable to guarantee the robust performance such as precise reference frequency tracking and disturbance attenuation under a wide range of area-load disturbances and possible contract scenarios.

Acknowledgment

The authors are grateful to Dr. V. Donde from university of Illinois (USA), Dr. Y.Y. Cao from university of Virginia (USA) and Prof. M. Ikeda from Osaka University (Japan) for their kind discussions. We would like to thank the reviewers for their constructive comments and suggestions.

(Manuscript received July 31, 2003,
revised Nov. 10, 2003)

References

(1) N. Jaleeli, D.N. Ewart, and L.H. Fink: "Understanding Automatic Generation Control", *IEEE Trans. Power Syst.*, Vol.7, No.3, pp.1106–1122 (1992)

(2) R.D. Chritie and A. Bose: "Load Frequency Control Issues in Power System Operation after Deregulation", *IEEE Trans. Power Syst.*, Vol.11, No.3, pp.1191–1200 (1996)

(3) A. PS. Meliopouls, G.J. Cokkinides, and A.G. Bakirtzis: "Load Frequency Control Service in a Deregulated Environment", Proc. of 31st Int. Conf. on System Sciences, USA, pp.24–31 (1998)

(4) B. Roffel and W.W. deBoer: "Analysis of power and frequency control requirements in view of increased decentralized production and market liberalization", Control Engineering Practice, Article in press (2002)

(5) A. Feliachi: "Reduced H_∞ Load Frequency Controller in a Deregulated Electric Power System Environment", Proc. of the Conference on Decision & Control, pp.3100–3101, California, USA (1997)

(6) H. Bevrani: "A novel approach for power system load frequency controller design", Proc. of IEEE/PES T&D Asia Pacific, pp.184–189, Yokohama, Japan (2002)

(7) J.M. Arroyo and A.J. Conejo: "Optimal response of a power generator to energy, AGC, and reserve pool-based markets", *IEEE Trans. Power Syst.*, Vol.17, No.2, pp.404–410 (2002)

(8) B.H. Bakken and O.S. Grande: "Automatic Generation Control in a Deregulated Power System", *IEEE Trans. Power Syst.*, Vol.13, No.4, pp.1401–1406 (1998)

(9) H. Bevrani, A. Rezazadeh, and M. Teshnehlab: "Comparison of Existing LFC Approaches in Deregulated Environment", Proc. of 5th IEE Int. Conf. on Power System Management and Control, pp.238–243, London, UK (2002)

(10) H. Singh and A. Paplexopoulos: "Competitive procurement of

ancillary services by an independent system operator", *IEEE Trans. Power Syst.*, Vol.14, No.2, pp.498–504 (1999)
(11) F. Liu, Y.H. Song, J. Ma, S. Mei, and Q. Lu: "Optimal load-frequency control in restructured power systems", *IEE Proc. Gener. Transm. Distrib.*, Vol.150, No.1, pp.87–95 (2003)
(12) H. Bevrani: "Robust Load Frequency Controller in a Deregulated Environment: A μ-synthesis Approach", Proc. of IEEE Int. Conf. on Control Applications, pp.616–621, USA (1999)
(13) H. Bevrani, Y. Mitani, and K. Tsuji: "Robust load frequency regulation in a new distributed generation environment", Proc. of IEEE-PES General Meeting (CD-ROM), Toronto, Canada (2003)
(14) A.S. Meliopoulos, G.J. Cokkinides, and A.G. Bakirtzis: "Load-frequency control in a deregulated environment", *Decision Support Systems*, Vol.24, pp.243–250 (1999)
(15) D. Rerkpreedapong, A. Hasanovic, and A. Feliachi: "Robust load frequency control using genetic algorithms and linear matrix inequalities", *IEEE Trans. Power Syst.*, Vol.18, No.2, pp.855–861 (2003)
(16) H. Bevrani, Y. Mitani, and K. Tsuji: "Sequential design of decentralized load-frequency controllers using μ-synthesis and analysis", *Energy Conversion & Management*, Vol.45, No.6, pp.865–881 (2004)
(17) B. Delfino, F. Fornari, and S. Massucco: "Load-frequency control and inadvertent interchange evaluation in restructured power systems", *IEE Proc.-Gener. Transm. Distrib.*, Vol.149, No.5, pp.607–614 (2002)
(18) J. Kumar, NG. K. Hoe, and G.B. Sheble: "AGC simulator for price-based operation, Part 1: A model", *IEEE Trans. Power Syst.*, Vol.2, No.12, pp.527–532 (1997)
(19) J. Kumar, NG. K. Hoe, and G.B. Sheble: "AGC simulator for price-based operation, case study results", *IEEE Trans. Power Syst.*, Vol.2, No.12, pp.533–538 (1997)
(20) V. Donde, M.A. Pai, and I.A. Hiskens: "Simulation and optimization in a AGC system after deregulation", *IEEE Trans. Power Syst.*, Vol.16, No.3, pp.481–489 (2001)
(21) O.I. Elgerd and C. Fosha: "Optimum megawatt-frequency control of multiarea electric energy systems", *IEEE Trans. Power Apparatus Syst.*, Vol.PAS-89, No.4, pp.556–563 (1970)
(22) C. Fosha and O.I. Elgerd: "The megawatt-frequency control problem: A new approach via optimal control", *IEEE Trans. Power Apparatus Syst.*, Vol.PAS-89, No.4, pp.563–577 (1970)
(23) P. Gahinet and P. Apkarian: "A linear matrix inequality approach to H_∞ control", *Int. J. Robust & Nonlinear Control*, Vol.4, pp.421–448 (1994)
(24) R.E. Skelton, J. Stoustrup, and T. Iwasaki: "The H_∞ control problem using static output feedback", *Int. J. Robust & Nonlinear Control*, Vol.4, pp.449–455 (1994)
(25) Y.Y. Cao, Y.X. Sun, and W.J. Mao: "Output feedback decentralized stabilization: ILMI approach", *Systems & Control Lett.*, Vol.35, pp.183–194 (1998)
(26) Y.Y. Cao and Y.X. Sun: "Static output feedback simultaneous stabilization: ILMI approach", *Int. J. Control*, Vol.70, No.5, pp.803–8144 (1998)
(27) Y.Y. Cao, J. Lam, Y.X. Sun, and W.J. Mao: "Static output feedback stabilization: an ILMI approach", *Automatica*, Vol.34, No.12, pp.1641–1645 (1998)
(28) P. Gahinet, A. Nemirovski, A.J. Laub, and M. Chilali: LMI Control Toolbox, The MathWorks, Inc. (1995)

Hassan Bevrani (Student Member) received his M.Sc. degree (first class honors) in Electrical Engineering from K. N. Toosi University of Technology, Tehran, Iran in 1997. He is currently a Ph.D. student at Osaka University. His special fields of interest included robust control and modern control applications in Power system and Power electronic industry. He is a student member of the Institute of Electrical Engineers of Japan, IEE, and IEEE.

Yasunori Mitani (Member) received his B.Sc., M.Sc., and Dr. of Engineering degrees in electrical engineering from Osaka University, Japan in 1981, 1983, and 1986 respectively. He joined the Department of Electrical Engineering of the same university in 1990. He is currently a professor in Kyushu Institute of Technology. His research interests are in the areas of analysis and control of power systems. He is a member of the Institute of Electrical Engineers of Japan, the Institute of Systems, Control and Information Engineers of Japan, and the IEEE.

Kiichiro Tsuji (Member) received his B.Sc. and M.Sc. degrees in electrical engineering from Osaka University, Japan, in 1966 and 1968, respectively, and his Ph.D. in systems engineering from Case Western Reserve University, Cleveland, Ohio in 1973. In 1973 he jointed the Department of Electrical Engineering, Osaka University, and is currently a professor at Osaka University. His research interests are in the areas of analysis, planning, and evaluation of energy systems, including electrical power systems. He is a member of the Institute of Electrical Engineers of Japan, the Japan Society of Energy and Resources, the Society of Instrument and Control Engineers, the Institute of Systems, Control and Information Engineers, and the IEEE.